International Journal Of Advances In
ENGINEERING, SCIENCE, COMMERCE, MANAGEMENT AND LAW
(IJAESCML)

ISSN (Online)
3048-8427
Vol. 3 | Issue 3
2026

www.ijaescml.com | internationaljournal1234@gmail.com | Peer Reviewed & Refereed Journal

[Comparative Study of Shaped Columns in High-Rise Buildings Subjected to Lateral Loads Using ETABS]

Aditi Pandey*[1], Dr. Rahul Kumar Satbhaiya*[2]

*[1] MTech Research Scholar, Civil Department, Infinity Management & Engineering College, Sagar

*[2]Guide and HOD, Civil Department, Infinity Management & Engineering College, Sagar

ABSTRACT

Architects increasingly ask that structural members disappear into the wall line, leaving rooms free of intruding corners. Specially shaped reinforced-concrete columns — L-, T- and plus-shaped sections whose limbs sit within the wall thickness — answer that demand directly. What is less obvious, and what this paper addresses, is that the same geometry redistributes material away from the section centroid and therefore changes the lateral stiffness, the mass participation and ultimately the way a tall frame answers wind and earthquake demand.

A twelve-storey (G+12) reinforced-concrete building measuring 63.20 m × 29.50 m in plan and 43.2 m in height was modelled in ETABS in three variants that are identical in plan, storey height, slab, beam, material and loading, and differ in one respect only: column cross-section. Model A uses conventional rectangular columns, Model B T-shaped columns and Model C plus-shaped columns. Each variant was analysed by the equivalent-static method and by response-spectrum dynamic analysis in accordance with the relevant Indian Standards, and the governing responses — maximum bending moment, storey shear, lateral displacement and inter-storey drift — were extracted at every storey. The governing rectangular column was additionally designed by hand as an independent check on the finite-element output.

Replacing rectangular columns with specially shaped sections improved every lateral response measured. Against the rectangular baseline, the plus-shaped model reduced the peak bending moment by 31.4%, the peak storey shear by 12.8% and the roof displacement from 88.84 mm to 64.90 mm, a reduction of 26.9%; the T-shaped model achieved intermediate gains of 11.2%, 10.8% and 25.5%. The distinction is sharpest in inter-storey drift, where the rectangular frame reached 0.74% at the first storey — above the 0.4% ceiling of IS 1893 (Part 1) — while both shaped-column frames remained at or below 0.20% throughout the height. The plus-shaped configuration, which distributes material symmetrically about both principal axes, therefore emerged as the most efficient arrangement for resisting lateral load while simultaneously releasing corner floor area, indicating that specially shaped columns are a technically sound and economically attractive alternative to rectangular columns in high-rise construction.

KEYWORDS: specially shaped columns; high-rise buildings; lateral loads; ETABS; response-spectrum analysis; inter-storey drift; storey shear; comparative structural analysis.

Received	Accepted	Published	Article Type
25/06/2026	10/08/2026	18/08/2026	Research Paper

International Journal Of Advances In
ENGINEERING, SCIENCE, COMMERCE, MANAGEMENT AND LAW
(IJAESCML)

ISSN (Online)
3048-8427
Vol. 3 | Issue 3
2026

www.ijaescml.com | internationaljournal1234@gmail.com | Peer Reviewed & Refereed Journal

Introduction

1.1 Background

Contemporary residential and commercial architecture places a high value on uninterrupted interior space. Where a conventional rectangular column meets a wall junction or a building corner, part of the section inevitably projects into the room, breaking the wall plane and complicating the placement of furniture and partitions. Specially shaped columns avoid this by folding the section into the wall itself: the limbs of an L-, T- or plus-shaped column occupy the wall thickness, so the room boundary remains flush and the full floor area stays usable.

The structural consequences run deeper than the architectural benefit. Because the limbs place concrete and reinforcement further from the section centroid, a shaped column of a given area has a different second moment of area, a different torsional response and a different contribution to the storey stiffness than the rectangular column it replaces. In a tall building, where lateral displacement and inter-storey drift govern serviceability, these differences are not marginal. Experimental and numerical work over the last decade has consistently found that well-detailed shaped sections can match or exceed the ductility and lateral capacity of equivalent rectangular sections [1], [2], and whole-building studies in ETABS have shown that the arrangement and section of the vertical members strongly condition the response of the frame as a whole [3].

A column carries compression collected from slabs and beams and delivers it to the foundation, but it almost never carries axial force alone; bending about one or both principal axes accompanies it. Columns are classified by reinforcement type (tied, spiral, composite), by the eccentricity of the applied load (axial, uniaxial, biaxial), by slenderness (short or long, according to whether the ratio of effective length to least lateral dimension falls below or above twelve), by cross-sectional shape and by constituent material. Under seismic excitation the demands of strength and ductility must be satisfied together, and geometrically irregular cross-sections such as the L, T and plus are only partially covered by the interaction charts and design aids that serve rectangular and circular sections. Finite-element building-analysis software removes that obstacle by allowing arbitrary sections to be modelled directly and competing configurations to be compared under identical demand — which is precisely the approach adopted here.

1.2 Lateral loads on tall frames

As a building becomes taller and more slender, lateral actions overtake gravity as the controlling design case. Gravity load accumulates roughly in proportion to height, but the overturning moment generated by a lateral pressure distribution grows far faster, and the dynamic modes excited by ground motion concentrate displacement toward the upper storeys. Two quantities summarise the resulting serviceability problem: the peak lateral displacement at roof level, and the inter-storey drift, meaning the relative horizontal movement between adjacent floors expressed as a fraction of the storey height. Drift is the more demanding of the two, because it governs damage to cladding, partitions, glazing and services long before the frame itself is threatened.

Earthquake loading is inertial: ground acceleration imparts forces proportional to the mass of each floor, modulated by the natural periods and mode shapes of the structure. A stiffer frame has shorter periods and therefore attracts a different — and in the flat portion of the design spectrum, generally more favourable — distribution of demand. Wind loading is by contrast an externally applied pressure that depends on terrain category, basic wind speed and exposure, and grows with height. Both actions are resisted by the vertical members and by the frame action mobilised between beams and columns, so the cross-sectional shape of the columns, which fixes their share of the storey stiffness, bears directly on the outcome.

1.3 Research significance and objectives

Although specially shaped columns are now widely built, the published evidence is unevenly distributed. Member-level laboratory studies are numerous and detailed but do not translate directly into storey-wise frame response, while the whole-building comparisons that do exist are concentrated in low- and medium-rise frames, where lateral effects are comparatively mild. A direct, storey-by-storey comparison of rectangular, T- and plus-shaped columns for a genuinely high-rise frame,

ISSN (Online)
3048-8427
Vol. 3 | Issue 3
2026

reporting bending moment, storey shear, displacement and drift together under identical lateral demand, is therefore still needed. This study supplies that comparison, with the following specific objectives:

- To model a G+12 reinforced-concrete frame in three configurations that differ only in column cross-section, so that shape is isolated as the single independent variable.
- To analyse each configuration under seismic and wind action using both the equivalent-static and the response-spectrum methods.
- To extract and compare the maximum bending moment, storey shear, lateral displacement and inter-storey drift at every storey level.
- To identify the most efficient configuration for lateral-load resistance and to validate the finite-element output against an independent manual design of the governing member.

2. Literature Review

2.1 Earlier investigations

Wang, Huang and Fu [4] tested three T-shaped steel-reinforced concrete columns under simultaneous high temperature and vertical load to reproduce fire conditions. Failure pattern, temperature field and fire resistance all proved sensitive to the axial-compression ratio and the load eccentricity; cracking intensified as either quantity rose, and specimens at an axial-compression ratio of 0.6 lost roughly 57% of the fire resistance recorded at a ratio of 0.2.

Paul and Varghese [5] modelled criss-cross shaped concrete columns joined by lacing bars, by a single stiffened vertical plate and by double vertical plates in ANSYS. Double-plate connection gave the highest capacity and lacing bars the lowest; capacity fell as the column lengthened and rose with plate width and with the degree of concrete confinement. Subhan [6] examined concrete-encased steel sections under reverse-cyclic, buckling and monotonic loading and found that the embedded steel core roughly doubled the lateral-load resistance and roughly tripled the monotonic capacity relative to a plain reinforced-concrete section.

Moving from members to frames, Navghare and Khedikar [7] compared rectangular, L- and T-shaped sections in a G+10 frame by response-spectrum analysis in ETABS. The L-shaped configuration attracted the greatest base shear in both principal directions yet displayed the smallest joint displacement, while the rectangular configuration showed the opposite pairing. Shivaranjitha and Naveen Kumar [8] replaced rectangular columns with Y-shaped columns in an eight-storey commercial building, gaining about 20.5% in available floor area and permitting a reduction of nearly 40% in column count, with the inclined limbs transferring axial load efficiently into the central stem. Yang, Liu and Huang [9] compared a specially shaped column frame with a rectangular frame of equal member area and attributed the greater stiffness of the shaped frame to its larger second moment of area; corner columns experienced combined biaxial bending and axial force under strong motion, but the code-designed shaped frame resisted the earthquake as effectively as its rectangular counterpart.

Shet and colleagues [10] constructed axial-force–moment interaction diagrams for C-shaped equal-legged columns using both ETABS and an analytical procedure, and traced the discrepancy between the two to the parabolic stress block assumed in hand calculation against the equivalent rectangular block adopted by the software — an observation directly relevant to the validation exercise reported later in this paper. Mathew and Krishnachandran [11] varied steel shape, column length and tube thickness in tubed steel-reinforced concrete columns, finding that each additional millimetre of tube thickness reduced deformation by about 8% under constant load. Wang, Wei and Zhang [12] combined testing with finite-element modelling to characterise stirrup confinement in L-shaped columns under repeated axial load, showing that confinement is strongest within the stirrup plane and decays as stirrup spacing increases.

Two studies bear particularly on economy. Agrawal and Pajgade [13] analysed G+14 commercial buildings with shaped columns, with and without shear walls, in seismic zone III, and reported that adding shear walls alongside the shaped columns reduced both displacement and drift while producing a more economical structure than the shaped-column frame alone. Gumble

ISSN (Online)
3048-8427
Vol. 3 | Issue 3
2026

and Pajgade [14] compared rectangular against specially shaped columns at four building heights using equivalent-static analysis and found the shaped-column buildings to be simultaneously stiffer, more generous in usable corner area and cheaper to build. A review by Ladvikar and Mundhada [15] reached a consistent conclusion across the literature available at that time. Further member-level work refined the picture. Zhou and co-workers [16] studied L-shaped columns assembled from concrete-filled steel tubes under eccentric load and proposed a simplified design expression resolving the eccentric load into three axial loadings carried by the constituent mono-columns, with predicted capacities agreeing closely with test data. Zhang and colleagues [17] examined the ductility of steel-reinforced concrete T-shaped columns under reversed cyclic loading, reporting that capacity fell as the shear-span ratio increased and ductility fell as the axial-compression ratio rose, with the displacement-ductility coefficient nonetheless exceeding three. Kareem and Mathew [18] analysed a G+8 space frame that was H-shaped in plan, built alternately with T-shaped and square columns, and found the T-shaped configuration to give smaller displacements and drifts while attracting greater base shear. Beck and Dória [19] approached the problem from a different direction, using a reliability-based procedure with a nonlinear finite-element model to assess whether the resistance curves of the Brazilian steel code deliver uniform safety across the permitted slenderness range.

2.2 Recent advances (2020–2026)

Attention over the last few years has shifted toward prefabrication, composite construction and retrofit. Chen and co-workers [20] tested prefabricated L-shaped concrete-filled steel-tube columns of rectangular multi-cell section under lateral load applied at 0°, +45° and +135°, and showed that loading direction significantly alters both the hysteretic response and the ductility — confirming that the biaxial character of corner shaped-columns cannot be treated as a secondary effect in seismic design. Zhang and colleagues [21] combined axial tests on ten T-shaped box-T section columns with parametric finite-element studies, characterised how limb plate slenderness governs the transition between local and global buckling, and proposed revised design curves.

On the retrofit side, Salah and co-authors [22] tested six half-scale L-shaped columns with 90° and 135° re-entrant corners and demonstrated that steel jacketing raises axial capacity by 26–29% when the jacket is left disconnected at the ends but by 68–79% when it is connected — a striking illustration of how sensitive shaped-column strengthening is to detailing. Han and colleagues [23] tested nine L-shaped CFST columns across different cross-sectional combinations and confinement levels and confirmed favourable seismic characteristics alongside efficient use of internal space. Zhao and co-workers [24] calibrated an ABAQUS model against existing tests and then analysed twenty-five cross-shaped concrete columns with built-in T-shaped steel and steel tubes, reproducing hysteretic curves, skeleton curves and failure modes to within about 10% and deriving a capacity-calculation method for the composite section.

Liu and colleagues [25] investigated the oblique seismic behaviour of L-shaped columns strengthened at the base with carbon-fibre-reinforced-polymer slabs, varying loading angle, strengthening scheme, stirrup ratio and axial-compression ratio, and showed that the strengthening improves capacity and ductility under obliquely applied action — the very loading direction that is most critical for corner columns. Lv, Yang and Lin [26] tested newly assembled precast beam–column joints reinforced with L-shaped steel bars and reported satisfactory energy dissipation and joint integrity. Wang and Chen [27] carried out a full-scale shaking-table test on a prefabricated L-shaped column concrete structure, finding that it remained elastic under a rare intensity-7 event and began to deform about both principal axes under a rare intensity-8 event, thereby satisfying current code requirements. Wang and co-authors [28] strengthened existing L-shaped columns with 100 mm and 150 mm wing walls and recorded increases in load-bearing capacity of up to 254%, with the benefit most pronounced at high axial-compression ratios. At the whole-building scale, Raju and co-workers [29] confirmed by dynamic analysis that discontinuities in the vertical load path sharply increase base shear and storey displacement, while Anjum and colleagues [30] evaluated a ten-storey reinforced-concrete building using both pushover and response-spectrum analysis in ETABS and underlined the role of higher modes in the drift response of taller frames.

ISSN (Online)
3048-8427
Vol. 3 | Issue 3
2026

2.3 Research gap

Taken together, and summarised in Table 1, the literature establishes three points with reasonable confidence: shaped columns can equal or surpass rectangular columns in stiffness, ductility and economy; their biaxial behaviour makes loading direction and limb proportion decisive; and detailing determines whether the theoretical advantage is realised. What remains missing is a systematic, storey-by-storey comparison for a genuinely high-rise frame in which all four governing lateral responses are reported together for the same building under the same loading. Most frame-level comparisons stop at ten or fewer storeys, and member-level studies, however rigorous, cannot supply storey-wise drift profiles. The present study addresses that gap for a G+12 frame.

Table 1. Summary of the reviewed literature on shaped columns

Reference(s)	Focus of the study	Principal finding
[4], [17]	T-shaped SRC columns (fire and cyclic loading)	Response governed by axial-compression and shear-span ratios.
[5], [6], [11]	Composite and encased-steel sections	Steel core and plate connection raise capacity and reduce deformation.
[7], [14], [15], [18]	Frame comparison, shaped vs rectangular	Shaped columns give smaller drift and prove more economical.
[8]	Y-shaped columns	About 20% more usable floor area; column count cut by 40%.
[9]	Seismic, shaped vs rectangular frame	Shaped frame stiffer; resists earthquake at least as well.
[10]	Pu–Mu interaction, C-shaped columns	Software–manual differences traced to stress-block assumption.
[12], [16], [23]	L-shaped RC and CFST columns	Good confinement and ductility; strongly biaxial behaviour.
[13]	Shaped columns with and without shear walls	Shear walls reduce displacement and drift, and lower cost.
[20], [25], [27], [28]	Prefabricated and retrofitted L-shaped (recent)	Loading direction critical; jacketing and wing walls raise capacity.
[21], [24]	Buckling and composite cross-sections (recent)	Limb slenderness governs buckling mode; FE models validated.
[3], [29], [30]	Whole-building ETABS studies (recent)	Section and layout strongly govern lateral response.

3. Building Configuration and Modelling

3.1 Rationale of the comparison

The credibility of a comparative study of this kind rests entirely on how well the variable of interest is isolated. Accordingly, a single reference building was adopted and reproduced in three variants that share plan dimensions, storey height, beam and slab sections, material grades, support conditions and applied loading. Only the column cross-section changes between them. Any difference in the computed response can therefore be attributed to shape, and not to some incidental difference in mass or geometry.

International Journal Of Advances In
ENGINEERING, SCIENCE, COMMERCE, MANAGEMENT AND LAW
(IJAESCML)
ISSN (Online)
3048-8427
Vol. 3 | Issue 3
2026
www.ijaescml.com | internationaljournal1234@gmail.com | Peer Reviewed & Refereed Journal

The reference structure is a twelve-storey (G+12) ordinary moment-resisting reinforced-concrete frame with an overall plan of 63.20 m × 29.50 m, a uniform floor-to-floor height of 3.6 m and a total height of 43.2 m, which is representative of high-rise residential construction in India. The three variants are:

- Model A — rectangular columns, 230 mm × 600 mm, serving as the baseline.
- Model B — T-shaped columns with limbs of 350 mm × 600 mm.
- Model C — plus-shaped columns with limbs of 350 mm × 750 mm.

The three cross-sections are drawn to a common scale in Figure 1, which makes the essential geometric distinction plain: the rectangular section concentrates material along one axis, the T-section adds a flange in the orthogonal direction, and the plus-section distributes material symmetrically about both principal axes.

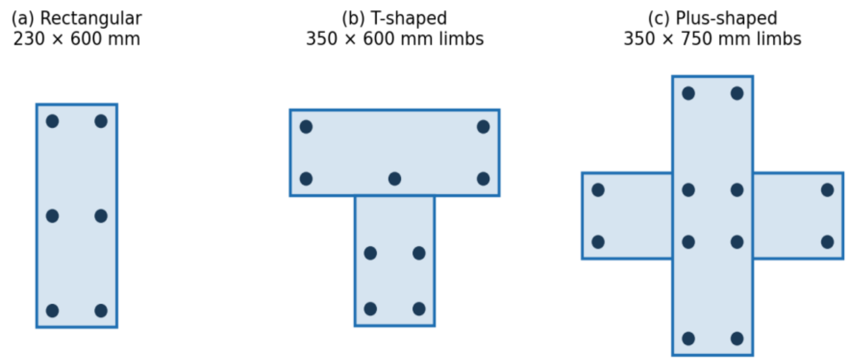

Figure 1. Column cross-sections compared in this study, drawn to a common scale: (a) rectangular, (b) T-shaped, (c) plus-shaped. Indicative longitudinal reinforcement is shown.

3.2 Geometry, materials and codes

The geometric and material data common to all three models are listed in Tables 2 and 3. Seismic design forces follow IS 1893 (Part 1) [31], gravity design follows IS 456 [32], and the load intensities are taken from IS 875 [33]. The building is located in seismic zone II on a medium (Type II) soil site.

Table 2. Geometric details and general data for the building models

Parameter	Value
Type of structure	Ordinary moment-resisting RC frame
Plan dimensions	63.20 m × 29.50 m
Number of storeys	G+12
Total height	43.2 m
Floor-to-floor height	3.6 m
Rectangular column (Model A)	230 mm × 600 mm
T-shaped column (Model B)	350 mm × 600 mm limbs
Plus-shaped column (Model C)	350 mm × 750 mm limbs
Beam section	300 mm × 500 mm
Slab thickness	200 mm
Wall thickness	230 mm
Grade of concrete	M 40
Grade of reinforcing steel	Fe 415

doi.org/10.5281/zenodo.22006916

International Journal Of Advances In
ENGINEERING, SCIENCE, COMMERCE, MANAGEMENT AND LAW
(IJAESCML)
ISSN (Online)
3048-8427
Vol. 3 | Issue 3
2026
www.ijaescml.com | internationaljournal1234@gmail.com | Peer Reviewed & Refereed Journal

Live load, floor / roof	3.0 / 1.5 kN/m²
Floor finish	1.0 kN/m²
Seismic zone / soil type	Zone II / Medium (Type II)
Support condition	Fixed at base

Table 3. Material properties adopted in the analysis

S. No.	Property	Value
1	Grade of concrete	M 40
2	Modulus of elasticity of concrete, Ec	2.17×10^4 N/mm²
3	Poisson's ratio of concrete	0.17
4	Density of concrete	25 kN/m³
5	Yield strength of reinforcing steel, fy	415 MPa
6	Ultimate tensile strength of steel	505 MPa
7	Modulus of elasticity of steel, Es	2.0×10^5 MPa

3.3 Loading

Four load cases were applied to each model: dead load, live load, earthquake load and wind load. Gravity loading is identical across the three models by construction; the lateral load cases are generated by the software from the assigned mass and stiffness and therefore differ between models, which is exactly the effect under investigation.

Dead load. Dead loads comprise the self-weight of the frame together with walls, parapets, finishes and permanent installations, evaluated in accordance with IS 875 (Part 1) [33]. The component values are computed in Table 4.

Table 4. Computation of dead loads

Component	Computation	Value	Unit
Wall load (h = 3.5 m)	0.18 × (3.5 − 0.4) × 18	10.00	kN/m
Parapet wall	0.18 × 1.2 × 18	5.00	kN/m
Slab self-weight (200 mm)	0.20 × 25	5.00	kN/m²
Floor finish	—	1.00	kN/m²

Live load. Imposed loads follow IS 875 (Part 2) [33]. A live load of 3.0 kN/m² is applied to typical floors and 1.5 kN/m² at roof level. For the purpose of computing the seismic mass, 0.75 kN/m² of the floor live load is included, as required by IS 1893 (Part 1) [31] for imposed loads not exceeding 3.0 kN/m².

Earthquake load. The seismic parameters are listed in Table 5. The approximate fundamental period was estimated from the empirical relation of IS 1893 (Part 1), Clause 7.6.2, in which $T = 0.09h/\sqrt{d}$, with h the height of the frame and d the base dimension in the direction considered. This yields 0.340 s in the X-direction and 0.420 s in the Z-direction. Both periods fall within the flat portion of the design spectrum for medium soil, for which the spectral acceleration coefficient Sa/g is 2.5.

Table 5. Seismic parameters adopted for the analysis

S. No.	Parameter	Value
1	Seismic zone and zone factor, Z	Zone II, Z = 0.10
2	Importance factor, I	1.0
3	Response reduction factor, R	5.0
4	Damping ratio	0.05
5	Soil / site type	Medium (Type II)
6	Spectral acceleration coefficient, Sa/g	2.5

ISSN (Online)
3048-8427
Vol. 3 | Issue 3
2026

7	Fundamental period, X-direction	0.340 s
8	Fundamental period, Z-direction	0.420 s

Wind load. Because the study concerns lateral loading in general rather than seismic action alone, wind was also considered, following IS 875 (Part 3) [33]. The parameters are given in Table 6. For a frame of this height in zone II the seismic case governs the lateral design, but retaining the wind case ensures that the comparison of column shapes is made against the full lateral-load envelope rather than a single action.

Table 6. Wind-load parameters adopted, to IS 875 (Part 3)

Parameter	Value
Basic wind speed, Vb	39 m/s
Terrain category	Category 2
Risk coefficient, k1	1.00
Terrain and height factor, k2	Varies with height
Topography factor, k3	1.00
Design wind pressure at 43.2 m	≈ 1.05 kN/m²

4. Methodology

4.1 Analysis platform

All modelling and analysis was carried out in ETABS, which is purpose-built for buildings and offers several features well matched to this study. Its object-based modelling treats slabs as area objects, beams and columns as line objects, and supports, masses and loads as point objects; its similar-storey facility allows repeated storeys to be edited simultaneously, which materially accelerates the construction of a twelve-storey frame. Most importantly for the present work, its Section Designer permits arbitrary cross-sections — including the T- and plus-shaped columns used here — to be defined and assigned in the same way as standard sections.

4.2 Analysis procedure

The following sequence was applied identically to each of the three models. The structural grid was laid out on the plan shown in Figure 2 and extruded through twelve storeys to produce the three-dimensional model of Figure 3. Supports were assigned as fixed at the base, and section properties were attached to beams, columns and slabs.

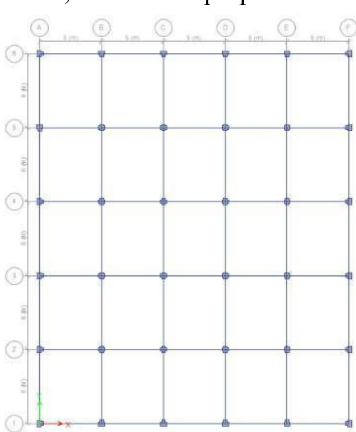

Figure 2. Structural grid and plan layout modelled in ETABS.

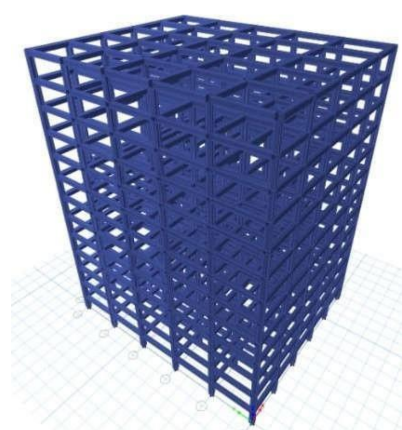

Figure 3. Three-dimensional ETABS model of the G+12 frame, identical in geometry across all three models.

doi.org/10.5281/zenodo.22006916

International Journal Of Advances In
ENGINEERING, SCIENCE, COMMERCE, MANAGEMENT AND LAW
(IJAESCML)

ISSN (Online)
3048-8427
Vol. 3 | Issue 3
2026

www.ijaescml.com | internationaljournal1234@gmail.com | Peer Reviewed & Refereed Journal

The rectangular columns of Model A were defined directly as frame sections. The T- and plus-shaped columns of Models B and C were built in the Section Designer, where the limb geometry and the longitudinal reinforcement layout were specified explicitly; the resulting sections are shown in Figure 4. Load patterns were then defined, the response-spectrum function was constructed in accordance with IS 1893 (Part 1) for zone II and medium soil with 5% damping (Figure 5), and the load combinations were assigned.

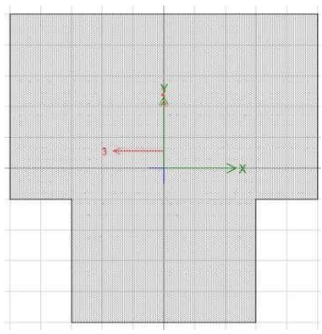

Figure 4 (a). T-shaped column in the ETABS Section Designer.

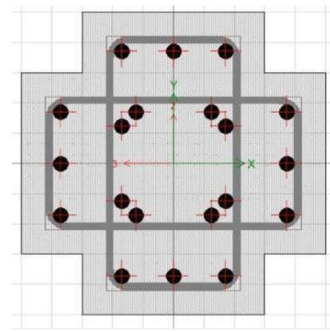

Figure 4 (b). Plus-shaped column, showing the doubly symmetric reinforcement arrangement.

Each model was then analysed for the static and dynamic load cases, and the storey-wise responses were extracted. Finally, the governing column of the baseline model was designed independently by hand as a check on the software output. The complete sequence is set out as a flowchart in Figure 6.

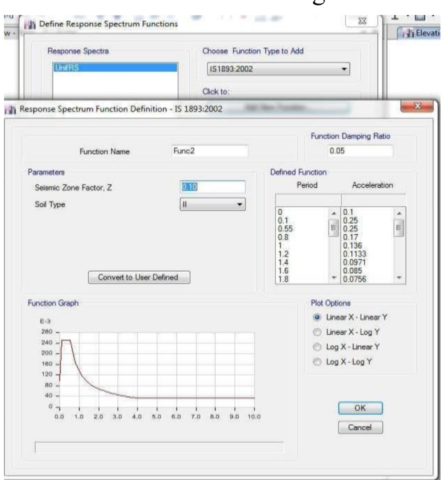

Figure 5. Definition of the IS 1893 response-spectrum function: zone factor Z = 0.10, soil type II, damping ratio 0.05.

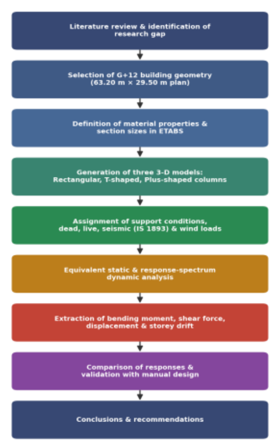

Figure 6. Flowchart of the research methodology adopted in this study.

5. Results and Discussion

The three models were analysed under identical loading and the four responses that govern the lateral design of a tall frame — maximum bending moment, storey shear, lateral displacement and inter-storey drift — were extracted at every storey. Throughout this section Model A (rectangular) serves as the baseline against which Models B and C are measured.

Table 7. Storey-wise maximum bending moment, storey shear and lateral displacement for the three column configurations

Storey	Maximum bending moment (kN·m)			Maximum storey shear (kN)			Maximum displacement (mm)		
	Rect.	T	Plus	Rect.	T	Plus	Rect.	T	Plus
12	826.76	734.17	566.81	941.85	840.43	821.54	88.84	66.16	64.90
11	814.58	705.63	553.84	923.25	813.87	797.91	83.19	60.46	58.52
10	789.44	677.09	540.87	904.65	787.31	771.23	77.54	54.76	51.22
9	770.21	648.55	527.90	886.05	760.75	748.90	71.89	49.06	46.31
8	719.30	620.01	514.93	867.45	734.19	712.45	66.24	43.36	39.67
7	698.67	591.47	501.96	848.85	707.63	694.77	60.59	37.66	32.90
6	675.20	562.93	488.99	830.25	681.07	672.85	54.94	31.96	27.71
5	629.10	534.39	476.02	811.65	654.51	637.31	49.29	26.26	21.48
4	559.89	505.85	463.05	793.05	627.95	619.21	43.64	20.56	17.54
3	578.90	477.31	450.08	774.45	601.39	583.36	37.99	14.86	11.76
2	524.99	468.00	437.11	755.85	574.83	554.45	32.34	9.16	7.87
1	510.22	461.05	424.14	737.25	548.27	528.77	26.69	3.46	1.21
Base	—	—	—	—	—	—	0.00	0.00	0.00

5.1 Maximum bending moment

Storey-wise bending moments are given in Table 7 and plotted in Figure 7. The moment is largest in the upper storeys, where lateral displacement and hence frame action are greatest, and decreases toward the base. At every level the ranking is consistent: rectangular columns attract the highest moment, T-shaped columns an intermediate value and plus-shaped columns the lowest. At the critical top storey the moment falls from 826.76 kN·m in Model A to 734.17 kN·m in Model B and 566.81 kN·m in Model C, a reduction of 31.4%.

The gradient of the three curves is also informative. The rectangular model varies irregularly with height, whereas the plus-shaped model produces an almost linear profile with a much gentler slope. A flatter moment envelope is desirable in practice because it allows a more uniform reinforcement arrangement over the height of the building, reducing both design effort and the risk of detailing error at storey transitions. The lower moment demand translates directly into a saving in flexural reinforcement.

International Journal Of Advances In
ENGINEERING, SCIENCE, COMMERCE, MANAGEMENT AND LAW
(IJAESCML)
ISSN (Online)
3048-8427
Vol. 3 | Issue 3
2026
www.ijaescml.com | internationaljournal1234@gmail.com | Peer Reviewed & Refereed Journal

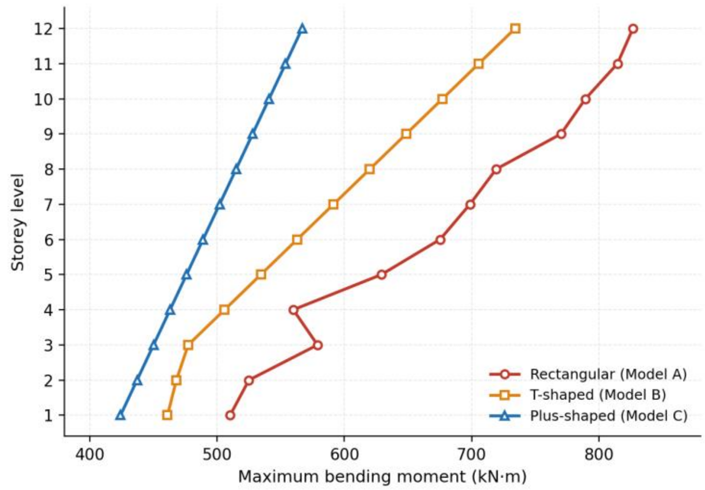

Figure 7. Variation of maximum bending moment along the height of the building.

5.2 Maximum storey shear

Storey shears are given in Table 7 and plotted in Figure 8. The distribution is the inverse of the moment profile: shear accumulates toward the base, where the total lateral force transmitted is greatest. Once again the rectangular model carries the highest shear at every level. At the top storey the shear falls from 941.85 kN in Model A to 840.43 kN in Model B and 821.54 kN in Model C, and the reductions persist down the full height, reaching 737.25 kN, 548.27 kN and 528.77 kN respectively at the first storey.

It is worth noting that the proportional benefit of the shaped columns is larger at the base than at the roof — about 28% at storey 1 against about 13% at storey 12 for the plus-shaped model. This is consistent with the stiffer shaped frames attracting a lateral force distribution that is less concentrated at the lower storeys, and it matters practically because base-storey shear governs the transverse reinforcement of the columns and the design of the foundation.

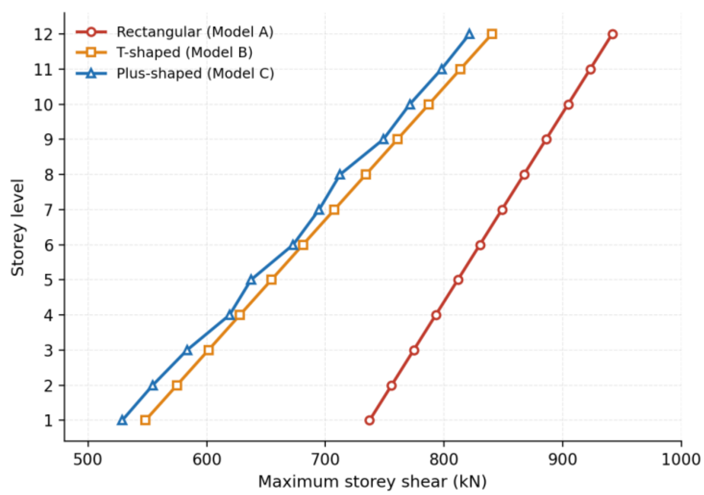

Figure 8. Variation of maximum storey shear along the height of the building.

5.3 Maximum storey displacement

Lateral displacements are given in Table 7 and plotted in Figure 9. Displacement increases monotonically with height in all three models and peaks at roof level, as expected for a moment-resisting frame. The roof displacement falls from 88.84 mm in Model A to 66.16 mm in Model B and 64.90 mm in Model C, reductions of 25.5% and 26.9% respectively.

The shape of the three profiles is more revealing than the peak values alone. The rectangular model displaces 26.69 mm at the first storey, whereas the T- and plus-shaped models displace only 3.46 mm and 1.21 mm at the same level. In other words, the rectangular frame accumulates almost 30% of its total roof displacement within the first storey, while the shaped-column frames distribute deformation far more evenly up the height. This near-linear displacement profile is characteristic of a frame with adequate lateral stiffness at the base, and it is the single clearest indication in these results that the shaped sections stiffen the structure where it matters most.

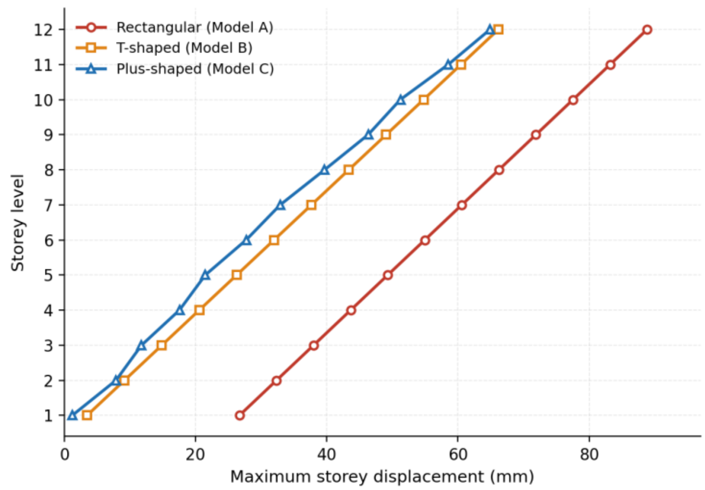

Figure 9. Maximum storey displacement profile for the three column configurations.

5.4 Inter-storey drift

Inter-storey drift — the relative displacement between adjacent floors divided by the storey height — is the response that most directly governs serviceability and damage to non-structural components. Drift ratios computed from the displacement data of Table 7, with a storey height of 3600 mm, are plotted in Figure 10.

The result is the most consequential finding of the study. The rectangular model reaches a drift ratio of 0.74% at the first storey, which exceeds the limit of 0.4% of the storey height stipulated by IS 1893 (Part 1) [31]. Above the first storey the rectangular model settles to a near-uniform 0.16% and is comfortably compliant. Both shaped-column models remain within the limit at every level without exception: the T-shaped model peaks at 0.16% and the plus-shaped model at 0.20%.

The rectangular model therefore fails the drift check at precisely the location where a soft-storey mechanism would be expected to initiate, while the shaped-column models pass it throughout. This is not a marginal difference in performance but a difference in code compliance, and it would require the rectangular scheme to be revised — by enlarging the ground-storey columns, adding shear walls or introducing bracing — before it could be built. Viewed in that light, the shaped columns are not merely an improvement on the baseline; for this particular frame they are what makes the frame work. The mild zig-zag visible in the plus-shaped drift profile, alternating between roughly 0.11% and 0.20%, is an artefact of the displacement values having been rounded before differencing rather than a physical irregularity in the frame.

International Journal Of Advances In
ENGINEERING, SCIENCE, COMMERCE, MANAGEMENT AND LAW
(IJAESCML)
ISSN (Online)
3048-8427
Vol. 3 | Issue 3
2026
www.ijaescml.com | internationaljournal1234@gmail.com | Peer Reviewed & Refereed Journal

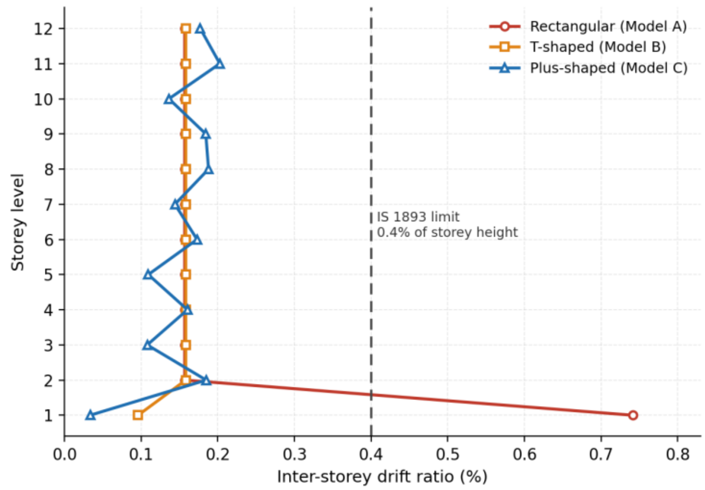

Figure 10. Inter-storey drift ratio along the height of the building, compared with the 0.4% limit of IS 1893 (Part 1).

5.5 Comparison of peak responses

The peak values of the three principal responses are collected in Table 8 and compared graphically in Figures 11 and 12. Every peak response is reduced relative to the rectangular baseline, and the plus-shaped configuration is the most effective overall, lowering the peak bending moment by 31.4%, the peak storey shear by 12.8% and the peak displacement by 26.9%. The T-shaped configuration delivers smaller but still substantial improvements of 11.2%, 10.8% and 25.5% respectively.

The pattern of these reductions repays attention. In displacement the two shaped sections perform almost identically — 25.5% against 26.9% — whereas in bending moment the plus-shaped section is nearly three times as effective as the T-shaped section. The explanation lies in the symmetry of the sections. Both shaped columns add material away from the centroid and so both stiffen the frame against translation, which is why the displacement gains are comparable. The plus-shaped section, however, is symmetric about both principal axes, so it offers that added stiffness equally in both directions and avoids the biaxial eccentricity that the singly-symmetric T-section introduces at wall junctions and corners. This is the mechanism identified in the earlier literature on the biaxial behaviour of shaped columns [9], [20], and the present whole-building results are consistent with it.

Axial force varied only marginally between the three models, as expected: gravity loading is identical by construction and the tributary areas are unchanged, so the axial demand on a given column is essentially independent of its shape.

Table 8. Peak response summary and reduction relative to rectangular columns

Response quantity	Rectangular	T-shaped	Plus-shaped
Peak bending moment (kN·m)	826.76	734.17	566.81
Reduction in bending moment (%)	—	11.2	31.4
Peak storey shear (kN)	941.85	840.43	821.54
Reduction in storey shear (%)	—	10.8	12.8
Peak displacement (mm)	88.84	66.16	64.90
Reduction in displacement (%)	—	25.5	26.9
Peak inter-storey drift (%)	0.74	0.16	0.20

International Journal Of Advances In
ENGINEERING, SCIENCE, COMMERCE, MANAGEMENT AND LAW
(IJAESCML)

ISSN (Online)
3048-8427
Vol. 3 | Issue 3
2026

www.ijaescml.com | internationaljournal1234@gmail.com | Peer Reviewed & Refereed Journal

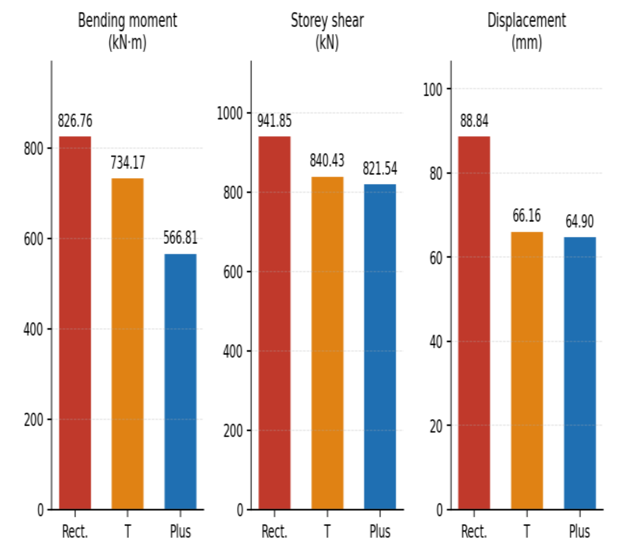

Figure 11. Peak structural responses by column shape.

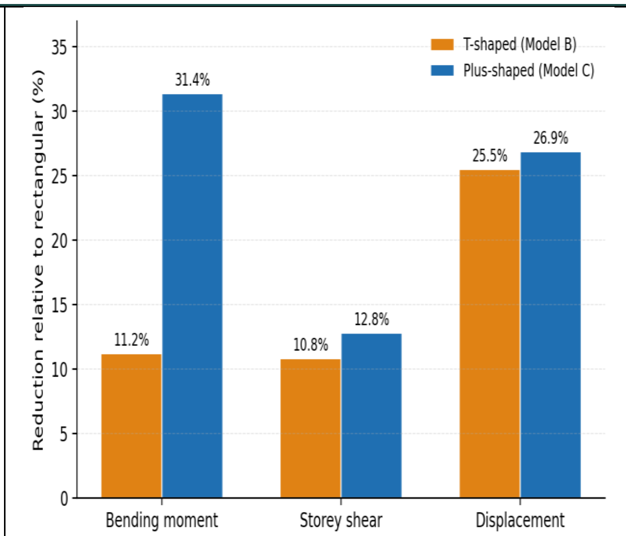

Figure 12. Percentage reduction in peak response relative to the rectangular baseline.

6. Validation Against Manual Design

To test the reliability of the finite-element output, the governing column of the rectangular model was designed independently by hand using the provisions of IS 456 [32] together with the design charts of SP 16 [34]. The comparison is given in Table 9. Agreement is excellent for the two responses that depend chiefly on global stiffness. The manual maximum displacement of 88.87 mm differs from the ETABS value of 88.84 mm by 0.03%, and the manual shear force of 935.43 kN differs from the software value of 941.85 kN by 0.68%. Both are well within any reasonable tolerance and confirm that the mass, stiffness and load path of the model have been assembled correctly.

The bending moment shows a larger discrepancy: 653.87 kN·m by hand against 826.76 kN·m from ETABS, a difference of 20.9%. This deserves to be stated plainly rather than glossed over. Two factors account for most of it. First, the hand calculation adopts the parabolic stress block of IS 456 whereas the software uses the equivalent rectangular (Whitney) block, a divergence that Shet and colleagues [10] identified as the principal source of disagreement between manual and ETABS results for shaped sections. Second, the manual check evaluates a single governing member under a design combination, while the software reports the envelope maximum across all combinations and all members at that storey, which is necessarily the larger figure. The manual result is therefore best read as a lower-bound confirmation that the software output is of the correct order and sign, rather than as an independent reproduction of it. Since the same modelling assumptions and the same envelope convention apply to all three models, this offset does not affect the comparative conclusions of the study, which rest on differences between models rather than on absolute magnitudes.

Table 9. Comparison of manual design with ETABS output for the governing column of Model A

Design quantity	ETABS	Manual	Difference
Maximum displacement (mm)	88.84	88.87	0.03%
Maximum shear force (kN)	941.85	935.43	0.68%
Maximum bending moment (kN·m)	826.76	653.87	20.9%
Maximum axial force (kN)	—	1062	—

7. Conclusions

International Journal Of Advances In
ENGINEERING, SCIENCE, COMMERCE, MANAGEMENT AND LAW
(IJAESCML)
ISSN (Online) 3048-8427
Vol. 3 | Issue 3
2026
www.ijaescml.com | internationaljournal1234@gmail.com | Peer Reviewed & Refereed Journal

This study compared a G+12 reinforced-concrete high-rise framed with rectangular, T-shaped and plus-shaped columns under identical lateral loading, using equivalent-static and response-spectrum analysis in ETABS. The principal conclusions are as follows.

- Bending moment. Specially shaped columns consistently attracted lower bending moments than rectangular columns at every storey. The peak moment fell from 826.76 kN·m to 734.17 kN·m for the T-shaped model and 566.81 kN·m for the plus-shaped model, a reduction of 31.4%, with a corresponding saving in flexural reinforcement.
- Storey shear. The peak storey shear reduced from 941.85 kN to 840.43 kN and 821.54 kN respectively, with the proportional benefit greatest at the base storey, where it approached 28% for the plus-shaped model.
- Lateral displacement. Roof displacement decreased from 88.84 mm to 66.16 mm and 64.90 mm, reductions of 25.5% and 26.9%. More significantly, the shaped-column models distributed deformation almost linearly up the height instead of concentrating it in the lower storeys.
- Inter-storey drift. The rectangular model reached 0.74% at the first storey and thus exceeded the 0.4% limit of IS 1893 (Part 1), whereas both shaped-column models remained at or below 0.20% throughout. For this frame the choice of column shape is therefore a question of code compliance, not merely of optimisation.
- Axial force. Axial demand was essentially unaffected by column shape, since gravity loading and tributary areas are identical across the models.
- Section symmetry. The plus-shaped column outperformed the T-shaped column most decisively in bending moment, where double symmetry avoids the biaxial eccentricity inherent in a singly-symmetric section, while the two performed comparably in displacement.
- Validation. Displacement and shear from the manual design agreed with ETABS to within 0.03% and 0.68% respectively. The 20.9% offset in bending moment is attributable to the differing stress-block assumptions and to the envelope convention of the software, and applies equally to all three models.

Taken together, these results indicate that specially shaped columns — and the plus-shaped section in particular — are a viable and economical alternative to rectangular columns in high-rise construction, delivering superior lateral performance while simultaneously releasing corner floor area for occupation.

8. Limitations and Future Scope

Several boundaries of the present work should be acknowledged, each of which suggests a direction for further study.

- The comparison covers a single building height in a single seismic zone. Extending it to taller frames, to higher seismic zones and to variable floor-to-floor heights would establish how the benefit of shaped columns scales.
- The three models were matched on plan geometry and loading rather than on column cross-sectional area, so the shaped sections carry somewhat more material than the rectangular baseline. A companion study matching sections on equal area, as Yang and colleagues [9] did at member level, would separate the contribution of shape from that of quantity.
- Analysis was linear-elastic. Nonlinear pushover and time-history analysis, together with P-delta effects, would allow performance-based assessment and reveal the collapse mechanism of each configuration.
- Seismic action governed this comparison. A fuller treatment of wind, including across-wind response and combined wind-and-seismic envelopes, would complete the lateral-load picture for very tall buildings.
- Cross-verification against an independent package such as SAP2000, and an explicit cost comparison of the three schemes including formwork and reinforcement, would strengthen the practical case. Comparative studies of alternative structural systems, such as that of Panchal and Marathe [35] on reinforced-concrete, steel and composite tall buildings, provide a useful template for such an exercise.

ISSN (Online)
3048-8427
Vol. 3 | Issue 3
2026

References

[1] W. Li, H. Ye, and L. Sun, "Experimental study on seismic behavior of T-shaped steel fiber reinforced concrete columns," Structural Concrete, vol. 24, no. 1, pp. 612–633, 2023. DOI: https://doi.org/10.1002/suco.202100666

[2] W. B. Ni, D. H. Qiao, H. W. Sun, et al., "Seismic performance of a full-scale precast concrete L-shaped column frame structure with a grouted connection," KSCE Journal of Civil Engineering, vol. 26, pp. 753–769, 2022. DOI: https://doi.org/10.1007/s12205-021-2159-2

[3] S. R. Kumar and P. Prasad, "A study of seismic analysis of building using ETABS for different plan configurations," International Journal of Innovative Research in Engineering and Management (IJIREM), vol. 10, no. 6, 2023. DOI: https://doi.org/10.55524/IJIREM.2023.10.6.2

[4] Y. Wang, Y. Huang, and C. Fu, "Performance of T-shaped steel reinforced concrete column under high temperature," in Proc. 6th Int. Workshop on Performance, Protection and Strengthening of Structures under Extreme Loading (PROTECT 2017), Guangzhou, China, Dec. 2017.

[5] M. P. Paul and N. Vargheese, "Axial compressive behaviour of criss-crossed shaped concrete columns fenced with steel," International Journal of Scientific and Engineering Research, vol. 10, no. 5, May 2019.

[6] Md. Subhan, "An investigational behaviour of RCC core steel composite column," SSRG International Journal of Civil Engineering, vol. 4, no. 5, May 2017.

[7] S. A. Navghare and A. Khedikar, "Analysis of RCC framed structure for column with modelling irregularities," International Journal of Innovative Research in Science, Engineering and Technology, vol. 6, Special Issue 11, May 2017.

[8] T. H. Shivaranjitha and S. Naveen Kumar, "Comparative study of Y-shaped columns with conventional rectangular shaped columns," International Research Journal of Engineering and Technology (IRJET), vol. 4, no. 6, June 2017.

[9] P. Yang, H. Liu, and Z. Huang, "A comparison of seismic behaviour between specially shaped column frame structure and rectangular column frame structures," in Proc. 14th World Conf. on Earthquake Engineering, Beijing, China, Oct. 2008.

[10] S. Shet, S. Shetty, and S. Shetty, "Analysis of Pu–Mu interaction diagram of C-shaped equal-legged RC column developed using ETABS and analytical method," International Journal of Engineering and Technology, vol. 7, no. 3.34, pp. 835–839, 2018.

[11] T. Mathew and V. N. Krishnachandran, "Parametric study on tubed steel reinforced concrete columns under axial loading," International Journal for Research in Applied Science and Engineering Technology (IJRASET), vol. 4, no. 8, Aug. 2016.

[12] X. Wang, S. Wei, and D. Zhang, "The finite element analysis of L-shaped concrete columns confined by stirrups under axial repeated loads," Advances in Engineering Research (AER), vol. 143, 2017.

[13] S. G. Agrawal and P. S. Pajgade, "Response of different shapes of columns on RC buildings with and without shear walls," International Journal of Innovative and Emerging Research in Engineering, vol. 3, Special Issue 1, 2016.

[14] A. N. Gumble and P. S. Pajgade, "Comparison between specially shaped columns and rectangular columns in R.C. structure," International Journal of Advance Engineering and Research Development, vol. 2, no. 5, May 2015.

[15] S. S. Ladvikar and A. R. Mundhada, "Effect of different column shapes on seismic performance of buildings: a review," International Journal for Research in Emerging Science and Technology, vol. 3, no. 12, Dec. 2016.

[16] T. Zhou, M. Y. Xu, Z. H. Chen, X. D. Wang, and Y. W. Wang, "Eccentric loading behavior of L-shaped columns composed of concrete-filled steel tubes," Advanced Steel Construction, vol. 12, no. 3, pp. 227–244, 2016.

[17] S. Zhang, S. Chen, Z. Li, and J. Zhang, "Research on hysteretic performance of steel reinforced concrete T-shaped column," MATEC Web of Conferences, 03003, 2016.

[18] S. M. Kareem and L. A. Mathew, "Seismic analysis of space frame with T and square shaped column," International Journal of Science and Research (IJSR), vol. 5, no. 7, July 2016.
[19] A. T. Beck and A. S. Dória, "Reliability analysis of I-section steel columns designed according to new Brazilian building codes," Journal of the Brazilian Society of Mechanical Sciences and Engineering, vol. 30, no. 2, Apr.–June 2008.
[20] H. R. Chen, L. Wang, H. T. Chen, and W. Cui, "Experimental study on the seismic behavior of prefabricated L-shaped concrete-filled steel tube with rectangular multi-cell columns under different lateral loading directions," Journal of Constructional Steel Research, vol. 177, 106480, 2021. DOI: https://doi.org/10.1016/j.jcsr.2020.106480
[21] Z. Zhang, G. Shi, S. Wang, and L. Zhou, "Investigation on buckling behavior of T-shaped box-T section columns under axial load," Engineering Structures, vol. 254, 113904, 2022. DOI: https://doi.org/10.1016/j.engstruct.2022.113904
[22] A. Salah, H. Elsanadedy, H. Abbas, T. Almusallam, and Y. Al-Salloum, "Behavior of axially loaded L-shaped RC columns strengthened using steel jacketing," Journal of Building Engineering, vol. 47, 103870, 2022. DOI: https://doi.org/10.1016/j.jobe.2021.103870
[23] D. Han, Z. Tao, W. Abdul Ghafar, M. M. Hasan, W. Xiao, T. Wang, K. Zhou, and H. Dai, "Experimental study on the seismic performance of L-shaped CFST columns in different combinations," Buildings, vol. 13, no. 9, 2320, 2023. DOI: https://doi.org/10.3390/buildings13092320
[24] L. Zhao, Y. Yu, C. Tang, L. Zhong, and Q. Qiu, "Seismic performance and bearing capacity calculation of cross shaped concrete columns with built-in T-shaped steel and steel tubes," PLoS ONE, vol. 18, no. 11, e0290426, 2023. DOI: https://doi.org/10.1371/journal.pone.0290426
[25] C. Liu, K. Luan, L. Wang, H. Wang, and J. Qin, "Study on the oblique seismic behavior of reinforced concrete L-shaped columns strengthened with carbon fiber reinforced polymer slabs," Structures, vol. 60, 105842, 2024. DOI: https://doi.org/10.1016/j.istruc.2023.105842
[26] M. Lv, T. Yang, and M. Lin, "Experimental study on seismic behavior of newly assembled concrete beam–column joints with L-shaped steel bars," Applied Sciences, vol. 14, no. 3, 1262, 2024. DOI: https://doi.org/10.3390/app14031262
[27] X. Wang and C. Chen, "Vibration table test of prefabricated L-shaped column concrete structure," Buildings, vol. 15, no. 13, 2329, 2025. DOI: https://doi.org/10.3390/buildings15132329
[28] W. Wang, J. Liao, Z. Li, M. Xie, C. Fang, M. Abdullah, and M. Zhang, "Seismic performance of existing reinforced concrete L-shaped columns strengthened with wing walls," Buildings, vol. 15, no. 20, 3645, 2025. DOI: https://doi.org/10.3390/buildings15203645
[29] T. H. Raju, V. R. S. Mandapati, A. Saxena, M. Gupta, Praveen, S. Zabibah Rahman, and B. Manideep, "Comparative study dynamics analysis of a multi-story building with and without a floating column," E3S Web of Conferences, vol. 552, 01133, 2024. DOI: https://doi.org/10.1051/e3sconf/202455201133
[30] N. Anjum, M. S. Rana, F. Islam, and M. A. Rahman, "Seismic performance evaluation of a 10-storey RC building using pushover analysis and response spectrum analysis," American Journal of Civil Engineering, vol. 14, no. 1, pp. 20–38, 2026. DOI: https://doi.org/10.11648/j.ajce.20261401.13
[31] Bureau of Indian Standards, IS 1893 (Part 1): 2016, Criteria for Earthquake Resistant Design of Structures — General Provisions and Buildings. New Delhi: BIS, 2016.
[32] Bureau of Indian Standards, IS 456: 2000, Plain and Reinforced Concrete — Code of Practice. New Delhi: BIS, 2000.
[33] Bureau of Indian Standards, IS 875 (Parts 1–3), Code of Practice for Design Loads (Dead, Imposed and Wind Loads) for Buildings and Structures. New Delhi: BIS.

ISSN (Online)
3048-8427
Vol. 3 | Issue 3
2026

[34] Bureau of Indian Standards, SP 16: 1980, Design Aids for Reinforced Concrete to IS 456. New Delhi: BIS, 1980.

[35] D. R. Panchal and P. M. Marathe, "Comparative study of RCC, steel and composite (G+30 storey) building," in Proc. National Conf. on Recent Trends in Engineering and Technology, Nirma University, Ahmedabad, India, 2011.